Analysis of a subgrid-scale model for turbulent condensation

By R. Paoli†, K. Shariff AND A. Shirgaonkar

A model for the condensation of a population of cloud droplets in a homogeneous turbulent flow is presented. The model consists of a set of Langevin (stochastic) equations for the droplet area, supersaturation, and temperature surrounding the droplets. These equations yield corresponding ordinary differential equations for various moments and correlations, and can be integrated exactly. The statistics predicted by the model, for instance the droplet area-supersaturation correlation, reproduce well those from available DNS of condensation in forced homogeneous turbulence. The application of the model as a closure for subgrid microphysics in LES of clouds is discussed.

1. Motivation and objectives

Interaction between turbulence and particles plays an important role in a number of cloud processes such as radiation scattering and absorption, precipitation efficiency, and heterogeneous chemical reactions (Shaw 2003). One challenging and still unsolved issue in the atmospheric science community (Cooper 1989, Pinsky & Khain 1997, Shaw 2003) is whether and how turbulence affects the evolution of the droplet size distribution $f(r, \mathbf{x}, t)$ in a cloud. This is the fundamental quantity in most cloud microphysics models (see Pruppacher & Klett 1997 for a review): it represents the density of particles that have a size between r and $r + dr$ in a neighborhood of a given point $\mathbf{x}$, at a given time t. Particle size distributions evolve according to a classical Boltzmann transport equation (see, e.g., Seinfeld & Pandis 1997)

$$\frac{\partial f}{\partial t} + \nabla \cdot (f\mathbf{u}) + \frac{\partial}{\partial r}(f\dot{r}) = K \tag{1.1}$$

where $\dot{r}$ and K are source terms for particle size growth and particle collisions, respectively. During the early stages of droplet growth, water vapor condensation on to the particle surface is the relevant microphysical process (particles are too small for collisions to be effective) and their growth can be described by the law (Seinfeld & Pandis 1997, Pruppacher & Klett 1997)

$$\dot{r} = \alpha\frac{S}{r}\,, \quad S = \rho_v - \rho_v^{sat}(T) \tag{1.2}$$

where temperature T, vapor mass fraction Y_v and density $\rho_v \equiv \rho Y_v$, and supersaturation S with respect to water are evaluated at the particle location. As suggested by Srivastava (1989) and Khvorostyanov & Curry (1999a), (1.1) and (1.2) show that, if turbulent fluctuations in temperature T' and vapor density Y_v' arise in a cloud, the resulting supersaturation fluctuations S' lead to different growth rates $\dot{r}'$ from particle-to-particle, thus affecting their size distribution $f(r)$. On the other hand, as large droplets consume more water vapor than small particles (see (1.3) below), supersaturation fluctuations are

† CERFACS, 42 Avenue Gaspard Corioils, 31057 Toulouse Cedex 1, France

N	L_e/L_{box}	Re_λ	$k_{max}\eta$	$\langle T\rangle$	$\langle Y_v\rangle$	σ_T	σ_{Y_v}
64	0.162	49	1.15	$292K$	0.014	0.3K	1.4×10^{-5}
128	0.162	69	1.68	$292K$	0.014	0.3K	1.4×10^{-5}

TABLE 1. Flowfield parameters of forced turbulence.

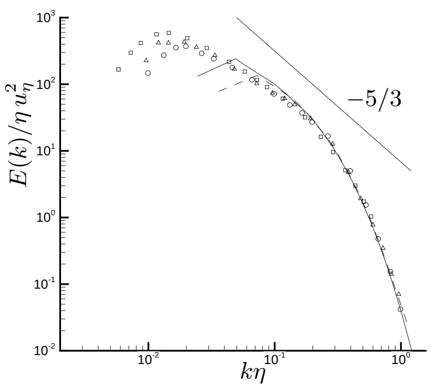

FIGURE 1. Average kinetic energy spectra normalized by the Kolmogorov length η and velocity u_η. Solid line: 128^3 simulation; dashed line: 64^3 simulation; symbols: $Re_\lambda \simeq 69$ grid-turbulence experiments of Comte-Bellot & Corrsin (1971).

in turn influenced by the particle size distribution. Applying this picture to a computational cell in a large-eddy simulation means that correlations such as $\overline{S'r'}, \overline{S'r^{2\prime}}$, etc., exist at the subgrid-scale level. The first of these correlations appears after applying an LES filter, denoted by an overbar, to the transport equation of vapor density (Paoli & Shariff 2003):

$$\frac{\partial\overline{\rho_v}}{\partial t} + \nabla\cdot\overline{\rho_v\mathbf{u}} - D_v\nabla\cdot(\overline{\rho\nabla Y_v}) = -n\overline{\dot{m}_w} = -4\pi n\rho_w\overline{r^2\dot{r}} = -4\pi n\rho_w\alpha\,\overline{rS}, \tag{1.3}$$

where n is the number density of droplets, $m_w \equiv 4/3\pi\rho_w r^3$ is the mass of a water droplet, and $\dot{m}_w$ represents the consumption of water vapor by condensation. Radius-supersaturation correlations also appear when one applies the method of moments to solve (1.1). To obtain evolution equations for the moments $m_k \equiv \int_0^\infty r^k f(r)dr$, one multiplies (1.1) by r^k and integrates in r. This results (Paoli *et al.* 2002) in unclosed terms of the type $\langle Sr^k\rangle$, where the angle brackets denote an ensemble average. Most LES codes used for cloud or contrail simulations usually neglect these correlations so that supersaturation is distributed uniformly over the computational cell. One major consequence of this assumption is that the particle size distribution is too narrow compared to what is observed e.g., in cumulus clouds (see for example Khvorostyanov & Curry 1999a, 1999b and Vaillancourt & Yau 2000).

The objective of this study is to propose a model for subgrid scale condensation that could be used to close subgrid scale correlations in LES of turbulent condensation. The model is based on a stochastic representation of condensation of a population of droplets.

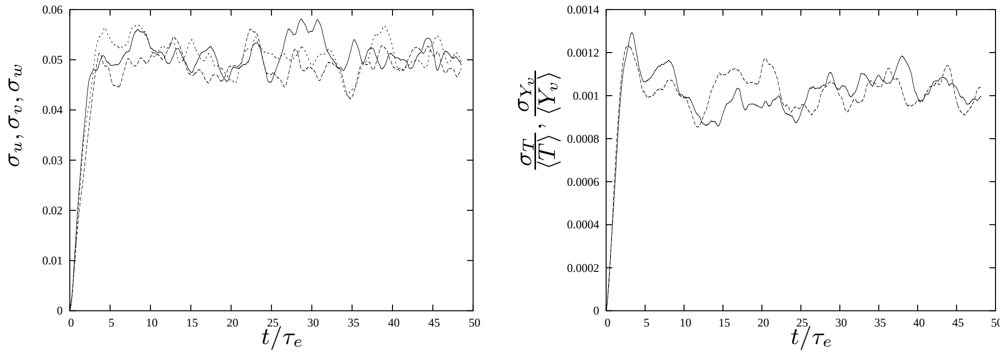

FIGURE 2. Forced turbulence: evolution of the standard deviations, normalized by the mean of the three componets of the velocity field (left), and temperature and vapor mass fraction (right).

For the sake of validation, we compare the correlations predicted by the model with those obtained from a DNS of turbulent condensation. The DNS database is described in Section 2, the derivation of the model and comparisons with DNS are shown in Section 3. Conclusions are provided in Section 4.

2. DNS database

Direct Numerical Simulations of turbulent condensation by Paoli and Shariff (2004) were used to test the model. The simulations were carried out using a mixed Eulerian/Lagrangian solver to treat the condensation of water vapor and the growth of cloud droplets in a box of turbulence. This was generated by forcing momentum, temperature, and water vapor equations with appropriate source terms designed to provide the desired level of fluctuations:

$$\frac{\partial \rho}{\partial t} + \frac{\partial (\rho u_j)}{\partial x_j} = 0 \tag{2.1}$$

$$\frac{\partial (\rho u_i)}{\partial t} + \frac{\partial (\rho u_i u_j)}{\partial x_j} + \frac{\partial p}{\partial x_i} = \frac{\partial \tau_{ij}}{\partial x_j} + \rho q_{f_i}, \; i = 1, \ldots, 3 \tag{2.2}$$

$$\frac{\partial (\rho T)}{\partial t} + \frac{\partial (\rho T u_j)}{\partial x_j} = \frac{\lambda}{c_v} \frac{\partial^2 T}{\partial x_j^2} + \rho q_T \tag{2.3}$$

$$\frac{\partial (\rho Y_v)}{\partial t} + \frac{\partial (\rho Y_v u_j)}{\partial x_j} = D_v \frac{\partial}{\partial x_j} \left(\rho \frac{\partial Y_v}{\partial x_j} \right) + \rho \omega_v + \rho q_{Y_v}. \tag{2.4}$$

Following the method proposed by Eswaran and Pope (1988), the source terms q_{f_i}, q_T, and q_{Y_v} are obtained as combinations of (low wavenumber) modes whose amplitudes are modeled as Ornstein-Uhlenbeck processes that satisfy appropriate Langevin equations (see e.g., Lemons 2002). Forcing parameters were designed to provide the correct energy spectrum and the desired levels of fluctuations for each of the forced variables. Figure 1 shows nice agreement of the simulated energy spectrum with the grid generated turbulence experiments of Comte-Bellot and Corrsin (1971), while Fig. 2 (right) and Table 1 show that temperature and vapor fluctuations are in the range of values observed in the atmosphere. For example, Kulmala *et al.* (1997) report $\sigma_{T_\infty} / \langle T_\infty \rangle = \sigma_{Y_{v_\infty}} / \langle Y_{v_\infty} \rangle \approx 0.001$. Droplets were inserted in the developed turbulent field at $t/\tau_e \simeq 50$ with uniform radius $r_0 = 5 \mu m$ while relative supersaturation was set to 0.5%, i.e., $Y_{v_0}/Y_{v_0}^s = 1.005$.

Particle trajectories were followed using a Lagrangian tracking approach and (1.2) was used to model droplet growth by vapor condensation. This approach provided direct computation of the particle ensemble averages and correlations that were used to validate the stochastic model derived in the following section. Given that our simulations are spatially homogeneous, an ensemble average at a given instant is obtained as an average over the population of droplets.

3. A model for stochastic condensation

Consider a population of N droplets in a parcel of volume VOL in a homogeneous turbulent cloud. For an inhomogeneous cloud, transport between parcels will need to be considered. Since droplet inertia is negligible (at least during the early stages of condensation), they behave as fluid particles, each carrying some scalar properties. Since the cloud is homogeneous, particles are uniformly distributed in a volume $\mathcal{V} = VOL/N \equiv 1/n$, which is the inverse of the number density. The model begins by assuming that temperature and vapor fluctuations around each droplet evolve according to two Langevin equations:

$$dT = -\frac{T - \langle T \rangle}{\tau_e}\, dt + \sqrt{2\sigma_{T_\infty}^2 \frac{dt}{\tau_e}}\, N_t^{t+dt}(0,1) \tag{3.1}$$

$$dY_v = -\frac{Y_v - \langle Y_v \rangle}{\tau_e}\, dt - \frac{n}{\rho}\, d\left(\frac{4}{3}\pi \rho_w\, r^3\right). \tag{3.2}$$

The first terms on both right-hand sides are the classical relaxation to the mean model with a time scale equal to the eddy turnover time τ_e (Pope 2000). The last term (3.2) accounts for loss of vapor by condensation. The last term in (3.1) is the Brownian motion associated to a Ornstein-Ulenbeck process and is supposed to model all processes like radiation that cannot be explicitly accounted for here. Brownian motions are random normal processes having the following properties:

$$\left\langle N_t^{t+dt}(0,1)\right\rangle = 0, \quad \left\langle [N_t^{t+dt}(0,1)]^2\right\rangle = 1, \quad \left\langle \varphi(t) N_t^{t+dt}(0,1)\right\rangle = 0 \tag{3.3}$$

for any continuous function $\varphi(t)$ (see Lemons 2002 for details). The formulation (3.1)–(3.2) gives the desired mean temperature $\langle T \rangle = T_\infty$ and variance $\sigma_T \to \sigma_{T_\infty}$ in the atmosphere. Saturation conditions are taken from the fit by Sonntag (1994):

$$p_v^s(T) = p X_v^s(T) = \exp\left(a_1 T^{-1} + a_2 + a_3 T + a_4 T^2 + a_5 \ln T\right) \tag{3.4}$$

$$Y_v^s = \frac{X_v^s}{X_v^s + (1 - X_v^s)\, W_{air}/W_v}. \tag{3.5}$$

As temperature fluctuations are small in the atmosphere ($\sigma_{T_\infty}/T_\infty \simeq 0.001$), one can expand $Y_v^s(T)$ around the ambient temperature T_∞. Expanding (3.4) around $T\infty$ and defining $\varphi_\infty = -a_1\, T_\infty^{-2} + a_3 + 2a_4\, T_\infty + a_5 T_\infty^{-1}$, yields after some algebra

$$Y_v^s(T) \simeq Y_v^s(T_\infty) + \left.\frac{dY_v^s}{dT}\right|_{T_\infty} (T - T_\infty) = Y_v^s(T_\infty)\,[1 + \varphi_\infty (T - T_\infty)]. \tag{3.6}$$

Substituting the latter into (3.1) with the help of (3.2) yields

$$dS = -\frac{S - \langle S \rangle}{\tau_e}\, dt + \sqrt{\beta_\infty^2 \frac{dt}{\tau_e}} N_t^{t+dt}(0,1) - \frac{4\pi n \rho_w}{3\rho}\, dr^3 \tag{3.7}$$

$$dr^2 = 2\alpha S\, dt \tag{3.8}$$

where we have defined $\beta_\infty^2 = 2\,\sigma_{T_\infty}^2 \varphi_\infty^2 Y_v^s(T_\infty)$. Due to the non-linearity of the condensation term in (3.7), no exact solutions can be obtained for the system of stochastic differential equations (3.7)–(3.8). However, consider the "surface area" $A \equiv r^2$ and assume its variation with respect to the instantaneous mean $\langle A \rangle$ is sufficiently small that the following approximation is valid:

$$r^3 \equiv A^{3/2} \simeq \langle A \rangle^{3/2} + \frac{3}{2} \langle A \rangle^{1/2} (A - \langle A \rangle) \;\Rightarrow\; dr^3 \equiv dA^{3/2} \simeq \frac{3}{2} \langle A \rangle^{1/2} dA. \tag{3.9}$$

Inserting (3.9) into (3.7), introducing the characteristic time for condensation $\langle \tau_c \rangle$ with respect to the mean radius (see, e.g., Khvorostyanov & Curry 1999a)

$$\langle \tau_c \rangle \equiv \frac{\Gamma}{4\pi n D_v \langle A \rangle^{1/2}} = \frac{\rho}{4\pi n \rho_w \alpha \langle A \rangle^{1/2}}, \tag{3.10}$$

finally yields

$$dS = -\frac{S - \langle S \rangle}{\tau_e} dt + \sqrt{\beta_\infty^2 \frac{dt}{\tau_e}} N_t^{t+dt}(0,1) - \frac{S}{\langle \tau_c \rangle} dt \tag{3.11}$$

$$dA = 2\alpha S\, dt. \tag{3.12}$$

3.1. *Evolution of mean quantities*

Taking the ensemble average of (3.11)–(3.12) yields

$$\frac{d \langle S \rangle}{dt} + \frac{\langle S \rangle}{\langle \tau_c \rangle} = 0 \tag{3.13}$$

$$\frac{d \langle A \rangle}{dt} = 2\alpha \langle S \rangle \tag{3.14}$$

where (3.3) was used. The above pair of equations can be easily solved numerically, however, if we make the expansion (3.9) about the initial mean $\langle A \rangle_0$, then closed form solutions can be written:

$$\langle A \rangle = \langle A \rangle_0 + 2\,\alpha \langle S \rangle_0 \langle \tau_c \rangle_0 \left(1 - e^{-t/\langle \tau_c \rangle_0}\right) \tag{3.15}$$

$$\langle S \rangle = \langle S \rangle_0\; e^{-t/\langle \tau_c \rangle_0}, \tag{3.16}$$

where $\langle \tau_c \rangle_0$ denotes the condensation time scale with respect to the initial size distribution.

3.2. *Evolution of auto-correlations*

We now examine the variances of S and A, taking care of the non-differentiable random function N. To compute $\langle S \rangle$ for example, we start from the differential form $dS^2 = S^2(t+dt) - S^2(t)$ as explained, for example, by Lemons (2002):

$$\begin{aligned} dS^2 &= \left[S(t) - \frac{S(t) - \langle S \rangle}{\tau_e} dt + \sqrt{\beta_\infty^2 \frac{dt}{\tau_e}} N_t^{t+dt}(0,1) - \frac{S}{\langle \tau_c \rangle} dt \right]^2 - S(t)^2 \\ &= \frac{\beta_\infty^2}{\tau_e} dt - 2S(t) \left(\frac{S(t) - \langle S \rangle}{\tau_e} \right) dt - 2\frac{S^2(t)}{\langle \tau_c \rangle} dt + \mathcal{O}(dt^{3/2}) \end{aligned}$$

where we used (3.3). Neglecting terms smaller than dt and taking the ensemble average yields

$$\frac{d \langle S^2 \rangle}{dt} + 2\left(\frac{1}{\tau_e} + \frac{1}{\langle \tau_c \rangle} \right) \langle S^2 \rangle = \frac{1}{\tau_e} \langle S \rangle^2 + \frac{\beta_\infty^2}{\tau_e}. \tag{3.17}$$

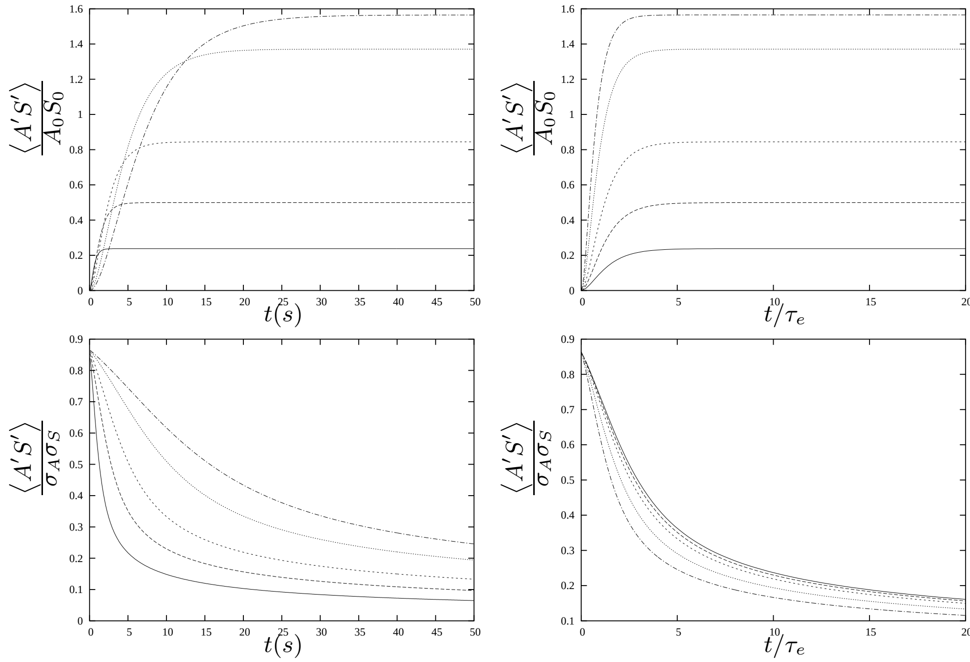

FIGURE 3. Evolution of model radius-supersaturation correlation: top, normalized correlation $\langle A'S' \rangle / A_0 S_0$; bottom, correlation coefficient $C_{AS} = \langle A'S' \rangle / \sigma_A \sigma_S$. Time is plotted in seconds in the two left plots, and scaled by τ_e in the two right plots. The different curves correspond to different τ_e from 0.4 seconds (solid line) to 20 seconds (dash-dotted line).

Again, this equation can also be solved numerically. However, replacing $\langle \tau_c \rangle$ with $\langle \tau_c \rangle_0$, using (3.16), and skipping the details of the computations, a closed form expression results for $\langle S^2 \rangle$ and $\sigma_S^2 \equiv \langle S^2 \rangle - \langle S \rangle^2$:

$$\langle S^2 \rangle = S_0^2 \, e^{-2t/\langle \tau_c \rangle_0} + \frac{\beta_\infty^2 / \tau_e}{2(1/\langle \tau_c \rangle_0 + 1/\tau_e)} \left[1 - e^{-2t(1/\langle \tau_c \rangle_0 + 1/\tau_e)} \right] \tag{3.18}$$

$$\sigma_S^2 = \frac{\beta_\infty^2 / \tau_e}{2(1/\langle \tau_c \rangle_0 + 1/\tau_e)} \left[1 - e^{-2t(1/\langle \tau_c \rangle_0 + 1/\tau_e)} \right] \tag{3.19}$$

3.3. *Evolution of the correlation* $< AS >$

We are interested in the $\langle AS \rangle$ correlation. Following the same method we write the differential $d(AS)$:

$$d(AS) \equiv A(t+dt)S(t+dt) - A(t)S(t) = -\frac{A(t)S(t) - A(t)\langle S \rangle}{\tau_e} \, dt$$
$$+ \sqrt{\beta_\infty^2 \frac{dt}{\tau_e}} A(t) N_t^{t+dt}(0,1) - \frac{1}{\langle \tau_c \rangle} A(t)S(t) \, dt + 2\alpha S^2(t) dt + \mathcal{O}(dt^{3/2}).$$

Averaging and using the relation $\langle A(t) N_t^{t+dt}(0,1) \rangle = 0$ gives

$$\frac{d\langle AS \rangle}{dt} + \left(\frac{1}{\tau_e} + \frac{1}{\langle \tau_c \rangle} \right) \langle AS \rangle = \frac{1}{\tau_e} \langle A \rangle \langle S \rangle + 2\alpha \langle S^2 \rangle . \tag{3.20}$$

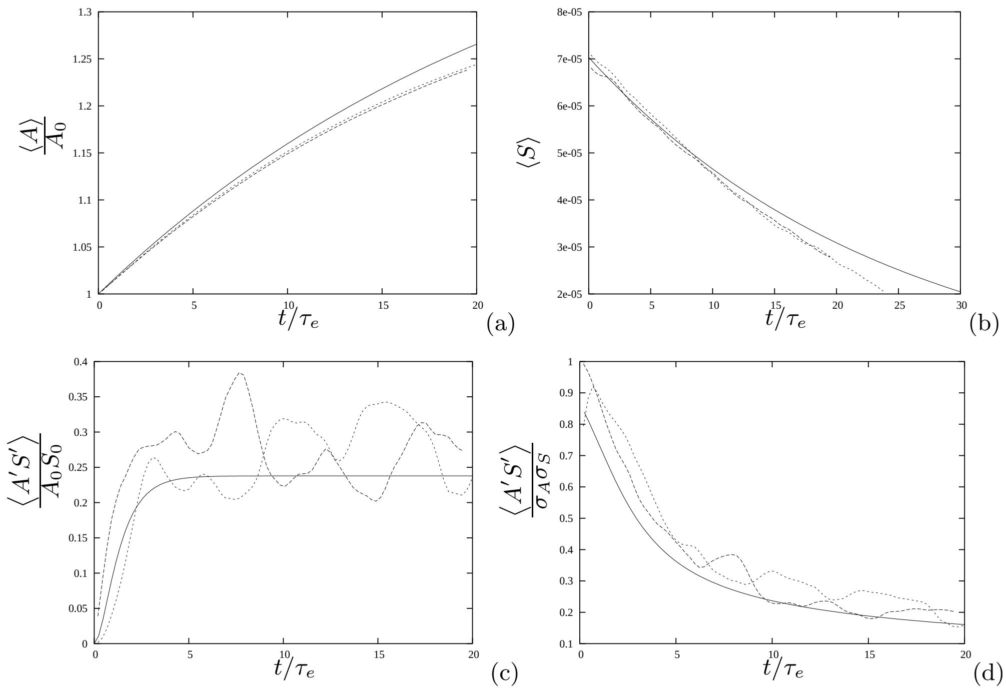

FIGURE 4. Comparison between the statistics predicted by the model (solid line) and the DNS statistics (dashed lines) obtained by forcing (2.3), and both (2.3) and (2.4), respectively (see Paoli and Shariff 2004): (a) normalized mean particle surface $\langle A\rangle$ (a); (b) mean supersaturation $\langle S\rangle$; (c) normalized correlation $\langle A'S'\rangle/A_0S_0$; (d) correlation coeffcient $C_{AS} = \langle A'S'\rangle/\sigma_A\sigma_S$.

Skipping again the details of the computations, the solution after setting $\langle\tau_c\rangle \approx \langle\tau_c\rangle_0$ is

$$\begin{aligned}\langle AS\rangle &= \langle A\rangle_0 \langle S\rangle_0\, e^{-t/\langle\tau_c\rangle_0} + 2\alpha\langle\tau_c\rangle_0 S_0^2\left(e^{-t/\langle\tau_c\rangle_0} - e^{-2t/\langle\tau_c\rangle_0}\right)\\ &+ \frac{\alpha\beta_\infty^2/\tau_e}{(1/\langle\tau_c\rangle_0 + 1/\tau_e)^2}\left[1 - 2e^{-t(1/\langle\tau_c\rangle_0+1/\tau_e)} + e^{-2t(1/\langle\tau_c\rangle_0+1/\tau_e)}\right]. \qquad (3.21)\end{aligned}$$

3.4. *Comparison of model predictions with DNS data*

The ensemble average statistics predicted by the model are summarized below for convenience:

$$\langle A\rangle = \langle A\rangle_0 + 2\alpha\langle S\rangle_0\langle\tau_c\rangle_0\left(1 - e^{-t/\langle\tau_c\rangle_0}\right)$$

$$\langle S\rangle = \langle S\rangle_0\, e^{-t/\langle\tau_c\rangle_0}$$

$$\sigma_S^2 = \frac{\beta_\infty^2/\tau_e}{2(1/\langle\tau_c\rangle_0 + 1/\tau_e)}\left[1 - e^{-2t(1/\langle\tau_c\rangle_0+1/\tau_e)}\right]$$

$$\sigma_A^2 = \frac{2\alpha^2\beta_\infty^2/\tau_e}{(1/\langle\tau_c\rangle_0 + 1/\tau_e)^3}\left[2t\,(1/\langle\tau_c\rangle_0 + 1/\tau_e) - 3 + 2e^{-t(1/\langle\tau_c\rangle_0+1/\tau_e)} - e^{-2t(1/\langle\tau_c\rangle_0+1/\tau_e)}\right]$$

$$\langle A'S'\rangle = \frac{\alpha\beta_\infty^2/\tau_e}{(1/\langle\tau_c\rangle_0 + 1/\tau_e)^2}\left[1 - 2e^{-t(1/\langle\tau_c\rangle_0+1/\tau_e)} + e^{-2t(1/\langle\tau_c\rangle_0+1/\tau_e)}\right].$$

Before comparing the model with the DNS, we did a parametric analysis of the model by varying τ_e, which is supposed to model the turbulent mixing in the cloud. For simplicity, we also assume an initial uniform supersaturation and droplet surface area, i.e., $\langle A\rangle_0 \equiv A_0$ and $\langle S\rangle_0 \equiv S_0$. This gives an initial characteristic condensation time $\langle\tau_c\rangle_0 \equiv \tau_{c0} \approx 10$ seconds. Figure 3 shows the evolution of the correlation coefficient $C_{AS} = \langle A'S'\rangle / \sigma_A \sigma_S$ for different τ_e ranging from 0.4 seconds (same as in the DNS) to 20 seconds. On dimensional arguments, it can be estimated as L_e/u_{rms} or K/ϵ, L_e, K and ϵ being the integral length scale, the turbulent kinetic energy and the dissipation rate in a cloudy parcel (or in a computational cell in the LES context).

In Fig. 4 we compare the model results with 64^3 DNS results. The model reproduces reasonably well the evolution of the mean surface area and supersaturation. Radius-supersaturation correlations are also well recovered for a few integral time scales. In particular, the model gives the correct trend of the decay law of C_{AS}, as well as the asymptotic value of $\langle A'S'\rangle$ correlation at $t/t_e \simeq 5$.

4. Conclusions

We presented a stochastic model for turbulent condensation, which could form a basis for a subgrid scale model for LES of clouds or contrails. The model reproduces the statistics obtained from previous DNS of condensation in forced homogeneous turbulence, where each droplet was tracked and correlations could be accurately measured. In particular, the model could recover the evolution of the area-supersaturation correlation, an important unclosed term in the filtered equation of water vapor density. This study represents a first attempt to model subgrid scale microphysics of clouds; the final goal will ultimately be to test the model in high Reynolds number LES of turbulent condensation in non-homogeneous flows.

REFERENCES

Comte-Bellot, G. & Corrsin, S. 1971 Simple Eulerian time correlation of full and narrow band velocity signals in isotropic turbulence. *J. Fluid Mech.*, **48**, 273–337.

Cooper, W. A. 1989 Effects of variable droplet growth histories on droplet size distributions. Part I: Theory. *J. Atmos. Sci.*, **46**, 1301–1311.

Eswaran, V. & Pope, S. B. 1988 An examination of forcing in direct numerical simulations of turbulence. *Comput. Fluids*, **16**, 257–278.

Khvorostyanov, V. I. & Curry, J. A. 1999a Toward the theory of stochastic condensation in clouds. Part I: A general kinetic equation. *J. Atmos. Sci.*, **56**, 3985–3996.

Khvorostyanov, V. I. & Curry, J. A. 1999b Toward the theory of stochastic condensation in clouds. Part II: Analytical solutions of the gamma-distribution type. *J. Atmos. Sci.*, **56**, 3997–4012.

Kulmala, M., Rannik, U., Zapadinsky, E., & Clement, C. 1997 The effect of saturation fluctuations on droplet growth. *J. Aerosol Sci.*, **28**, 1395–1409.

Lemons, D. S. 2002 *An Introduction to Stochastic Processes in Physics*. The Johns Hopkins University Press.

Paoli, R., Hélie, J., Poinsot, T. & Ghosal, S. 2002 Contrail formation in aircraft wakes using large eddy simulation. *Proceedings of the 2002 Summer Program*, Center for Turbulence Research, NASA Ames/Stanford Univ.

Paoli, R. & Shariff, K. 2003 Particle size distributions in atmospheric clouds. *Annual Research Briefs 2003*, Center for Turbulence Research, NASA Ames/Stanford Univ.

Paoli, R. & Shariff, K. 2004 Direct numerical simulation of turbulent condensation in clouds. *Annual Research Briefs 2004*, Center for Turbulence Research, NASA Ames/Stanford Univ.

Pope, S. B. 2000 *Turbulent Flows*, Cambridge University Press.

Pruppacher, H. R. & Klett, J. D. 1997 *Microphysics of Clouds and Precipitation.* Kluwer Academic Publishers, Dordrecht, The Netherlands.

Shaw, R. A. 2003 Particle-Turbulence Interactions in Atmospheric Clouds. *Annu. Rev. Fluid Mech.* **35**, 183-227.

Seinfeld, J. N. & Pandis, S. N. 1997 *Atmospheric Chemistry and Physics: From Air Pollution to Climate Change*, John Wiley & Sons Inc.

Sonntag, D. 1994 Advancements in the field of hygrometry. *Meteorol. Z.*, **3**, 51–66.

Srivastava, R. C. 1989 Growth of cloud Drops by Condensation: A criticism of currently accepted theory and a new approach. *J. Atmos. Sci.*, **46**, 869–887.

Vaillancourt, P. A. & Yau, M. K. 2000 Review of Particle-Turbulence Interactions and Consequences for Cloud Physics. *Bull. Am. Meteorol. Soc.*, **81**, 285–298.